Review Paper

The Canadian Biomarker Integration Network in Depression (CAN-BIND): magnetic resonance imaging protocols

Glenda M. MacQueen, MD, PhD*; Stefanie Hassel, PhD*; Stephen R. Arnott, PhD; Jean Addington, PhD; Christopher R. Bowie, PhD; Signe L. Bray, PhD; Andrew D. Davis, PhD; Jonathan Downar, MD, PhD; Jane A. Foster, PhD; Benicio N. Frey, MD, PhD; Benjamin I. Goldstein, MD, PhD; Geoffrey B. Hall, PhD; Kate L. Harkness, PhD; Jacqueline Harris, MSc; Raymond W. Lam, MD; Catherine Lebel, PhD; Roumen Milev, MD, PhD; Daniel J. Müller, MD, PhD; Sagar V. Parikh, MD; Sakina Rizvi, PhD; Susan Rotzinger, PhD; Gulshan B. Sharma, PhD, MBA; Claudio N. Soares MD, PhD, MBA; Gustavo Turecki, MD, PhD; Fidel Vila-Rodriguez, MD; Joanna Yu, PhD; Mojdeh Zamyadi, MSc; Stephen C. Strother, PhD; Sidney H. Kennedy, MD; on behalf of the CAN-BIND Investigator Team

Studies of clinical populations that combine MRI data generated at multiple sites are increasingly common. The Canadian Biomarker Integration Network in Depression (CAN-BIND; www.canbind.ca) is a national depression research program that includes multimodal neuroimaging collected at several sites across Canada. The purpose of the current paper is to provide detailed information on the imaging protocols used in a number of CAN-BIND studies. The CAN-BIND program implemented a series of platform-specific MRI protocols, including a suite of prescribed structural and functional MRI sequences supported by real-time monitoring for adherence and quality control. The imaging data are retained in an established informatics and databasing platform. Approximately 1300 participants are being recruited, including almost 1000 with depression. These include participants treated with antidepressant medications, transcranial magnetic stimulation, cognitive behavioural therapy and cognitive remediation therapy. Our ability to analyze the large number of imaging variables available may be limited by the sample size of the substudies. The CAN-BIND program includes a multimodal imaging database supported by extensive clinical, demographic, neuropsychological and biological data from people with major depression. It is a resource for Canadian investigators who are interested in understanding whether aspects of neuroimaging — alone or in combination with other variables — can predict the outcomes of various treatment modalities.

Introduction

Treatment of major depressive disorder (MDD) is evidence-based, but treatment selection is not personalized to the features of an individual's illness.[1] The discovery of biomarkers — or predictors — of treatment response is a priority in MDD research.[2] A major challenge for identifying patient characteristics that predict treatment response is that MDD is a complex, heterogeneous condition. Current diagnostic systems codify depressive symptoms as criteria for MDD,[3] but these symptoms are not unique to depression and, even if clustered together, they may not represent a single underlying disease process or treatment substrate.

A growing number of clinical studies are using MRI in an attempt to identify biomarkers of disease (for example, Jack and colleagues[4]), including depression (see Fonseka and colleagues[5] for a recent review of studies using MRI to define markers of outcome in MDD). One approach to the detection of imaging biomarkers is to integrate data from large numbers of patients collected in independent studies. Keshavan and colleagues[6] examined the circumstances under which a study could forgo efforts at protocol harmonization and

Correspondence to: G.M. MacQueen, 7th Floor, TRW Building, Cumming School of Medicine, 3280 Hospital Dr NW, Calgary, AB T2N 4Z6; gmmacque@ucalgary.ca

*These authors share first authorship.

Submitted Mar. 11, 2018; Revised Jul. 23, 2018; Revised Oct. 15, 2018; Accepted Oct. 18, 2018; Published online Mar. 6, 2019

DOI: 10.1503/jpn.180036

phantom-based correction, relying only on the power of the data. They performed a scan–rescan study on 20 scanners with similar but nonidentical imaging parameters and determined that, in the absence of protocol harmonization, the sample size required could be in the thousands. The Enhancing NeuroImaging Genetics through Meta-Analysis (ENIGMA) consortium is a collaborative network of researchers who have integrated primarily structural data from more than 12 000 participants and 70 institutions around the world.[7] The ENIGMA consortium has a working group focused on MDD that has reported on both subcortical[8] and cortical brain structures.[9] However, despite the power of this approach to examine factors such as age of onset and recurrence, ENIGMA's psychiatric cohorts vary in terms of inclusion and exclusion criteria, duration of illness, the absence or presence of comorbid conditions, treatment history, ethnicity and other factors, limiting investigators' ability to examine imaging data in the context of relevant clinical variables.[9]

An alternative approach to combining data from multiple independent studies is to conduct coordinated, multisite imaging studies. Several consortia have established guidelines and protocols for such studies, including the Function Biomedical Informatics Research Network (fBIRN),[10] the Alzheimer's Disease Neuroimaging Initiative (ADNI),[4,11] the Mind Clinical Imaging Consortium (MCIC),[12] the North American Imaging in Multiple Sclerosis (NAIMS) Cooperative[13] and the Ontario Neurodegenerative Disease Research Initiative (ONDRI).[14] However, only a few studies to date have employed multimodal, multisite imaging analyses to predict treatment outcomes in MDD.

The international Study to Predict Optimized Treatment in Depression (iSPOT)[15] enrolled more than 2000 patients with MDD across 20 sites, but they recruited only 10% of the participants into the neuroimaging substudy, which was conducted at 2 sites.[15,16] The iSPOT neuroimaging protocol included high-resolution 3-dimensional T_1-weighted scans; diffusion tensor imaging (DTI); and T_2-weighted proton density scans, as well as task-based functional MRI (fMRI) sequences to assess cognitive and emotional processing.[16] The Establishing Moderators and Biosignatures of Antidepressant Response in Clinical Care (EMBARC) study[17] enrolled 309 patients with early-onset MDD across 6 sites. The EMBARC neuroimaging protocol included 3-dimensional T_1-weighted scans, DTI, arterial spin labelling and task-based fMRI sequences to assess the processing of reward and emotional conflict.

The Canadian Biomarker Integration Network in Depression (CAN-BIND; www.canbind.ca; see Kennedy and colleagues[18] and Lam and colleagues[19]) is a national program in depression research, funded by the Ontario Brain Institute, that seeks to address remaining gaps in the literature on response prediction by scanning approximately 1000 patients with depression or risk for depression. The CAN-BIND program includes multiple projects and has recruited approximately 1300 participants to date, including about 1000 with depression and 300 healthy participants for comparison. The CAN-BIND neuroimaging platform relies on evidence that data from different scanners are sufficiently robust to provide comparable results across multiple sites.[20–23] Below, we briefly outline the substudies that use CAN-BIND imaging protocols.

The CAN-BIND-1 study includes 211 patients with MDD and 112 healthy controls. Medication-free patients were treated in an open trial protocol for 8 weeks with escitalopram, a selective serotonin reuptake inhibitor (SSRI). Nonresponders then had aripiprazole (an atypical antipsychotic) added to their regimen, and responders continued with escitalopram monotherapy for an additional 8 weeks (see Lam and colleagues[19] for a detailed description). The study included MRI at baseline and after 2 and 8 weeks of treatment. It recruited participants from 6 sites in Canada (ClinicalTrials.gov identifier NCT01655706).

The CAN-BIND-2 study (Canadian rTMS Treatment and Biomarker Network in Depression; CARTBIND) explored the use of repetitive transcranial magnetic stimulation (rTMS), a noninvasive brain stimulation technique approved as a treatment for MDD. The CARTBIND trial is a 3-site study that uses 6 weeks of left dorsolateral prefrontal cortex intermittent theta-burst rTMS in patients with MDD, with the aim of identifying biomarkers of response to rTMS treatment. Scans have been obtained for 205 patients at baseline and within 1 week of completing rTMS therapy (ClinicalTrials.gov identifier NCT02729792).

The CAN-BIND-3 study (Canadian Psychiatric Risk and Outcome Study; PROCAN) is a 2-site study with the goal of improving the ability to identify youth at risk of serious mental illness, including MDD.[24] In this study, 240 youth have been recruited, aged 12 to 25 years and at various levels of risk as defined in clinical staging models[25] (e.g., genetic risk only, mild and/or attenuated symptoms, more pronounced but subthreshold symptoms). Participants are scanned at baseline and at 1- and 2-year follow-up, or when symptoms worsen.

The CAN-BIND-4 (Stress and Reward Anhedonia; SARA) single-site study aims to examine stress reactivity and reward responsivity as correlated domains of functioning in depression in 200 participants (100 patients with MDD, 100 healthy controls). Structural and functional brain imaging is being obtained at baseline and 6-month follow-up.

The CAN-BIND-5 (Biomarkers of Suicidality) single-site study has the goal of identifying an integrated biological marker model to predict risk of suicide attempt in MDD, and to test the stability of this model over time. Ninety patients with MDD with and without a history of suicide attempt, as well as 30 healthy controls, are being scanned at a baseline visit and at 1-year follow-up (ClinicalTrials.gov identifier NCT02811198).

The CAN-BIND-9 (Remote Cognitive Remediation for Depression; ReCoRD) single-site study aims to assess the effectiveness of cognitive remediation therapy in 75 participants with MDD who complete computer treatment modules from their homes. Participants are scanned at baseline and after online cognitive remediation, at 12- and 24-week follow-up.

The CAN-BIND-10 (Concussion and Depression Study) single-site study aims to characterize the biological profile of people with mild traumatic brain injury and depression, and

to identify factors that may predict risk of depression after injury. Overall, 100 patients and 25 healthy controls are being scanned at entry into the study.

CAN-BIND participants

Participants are being recruited at 7 Canadian clinical centres: the University Health Network, the Centre for Addiction and Mental Health and Sunnybrook Health Sciences Centre in Toronto, Ontario; St. Joseph's Healthcare in Hamilton, Ontario; Providence Care Hospital in Kingston, Ontario; Djavad Mowafaghian Centre for Brain Health in Vancouver, British Columbia; and the Mathison Centre for Mental Health Research and Education in the Hotchkiss Brain Institute, Calgary, Alberta. Each site has entered a standardized participation agreement with the Ontario Brain Institute to facilitate the transfer of both raw and processed/deidentified data, in accordance with the Ontario Brain Institute's governance policy (www.braincode.ca/content/governance) and with any specific conditions required by each institution's local legislative and ethical policies.

For all studies except CAN-BIND-3 and CAN-BIND-10, patients have a primary diagnosis of MDD, based on structured clinical interview. The CAN-BIND-3[24] study includes youth aged 12 to 15 years at varying degrees of risk for serious mental illness as defined by a clinical staging model.[25] The CAN-BIND-10 study is recruiting patients with traumatic brain injury only and patients with both traumatic brain injury and MDD.

Across all studies, healthy participants for comparison have no history of psychiatric illness or current psychiatric illness as assessed by structured interview. Both patients and healthy participants are excluded if they have an estimated IQ of less than 70 based on the North American Adult Reading Test[26]; neurologic disease; a history of skull fracture or a severe or disabling medical condition; or a contraindication for MRI. Complete inclusion and exclusion criteria are specific to the various substudies.

CAN-BIND imaging protocols

The CAN-BIND program includes multiple longitudinal studies that employ common neuroimaging elements. Some use additional tasks and modalities, as indicated by the nature of the study. For the main characteristics and protocols for each CAN-BIND study, see Table 1, Table 2 and Appendix 1, Table S1 and Table S2. available at jpn.ca/180036.

The CAN-BIND protocols include the following imaging sequences: a high-resolution 3-dimensional isotropic T_1-weighted scan to assess fine anatomical detail and map cortical thickness; DTI to assess microstructural and

Table 1: Overview of CAN-BIND studies highlighting common, standardized data elements

CAN-BIND study*	CAN-BIND-1†	CAN-BIND-2	CAN-BIND-3	CAN-BIND-4	CAN-BIND-5	CAN-BIND-9	CAN-BIND-10
Characteristic	Drug	rTMS	At-risk youth	Stress and reward	Suicide markers	Cognitive remediation	TBI
Patient-specific information, diagnosis	MDD	MDD	Youth at risk for severe mental illness; family high risk	MDD	MDD, MDD with suicidal ideation or attempt	MDD	MDD, TBI, MDD + TBI
Intervention/treatment	SSRI (escitalopram); aripiprazole	rTMS	NA	NA	NA	Cognitive remediation therapy	NA
Patients, *n*	211	205	200	100	90	75	100
Controls, *n*	112	NA	40	100	30	NA	25
Number of times scanned	3	2	3	2	2	3	1
T_1 structural*	♦	♦	♦	♦	♦	♦	♦
Diffusion tensor imaging	♦	♦	♦	♦	♦	♦	♦
Resting-state fMRI	♦	♦	♦	♦	♦	♦	♦
Go/no-go task	♦	♦	♦	♦		♦	
Incentive delay task	♦	♦	♦	♦			
Working memory task			♦			♦	
Breath-holding challenge / breath-hold task					♦		♦
Shifted attention emotion appraisal test					♦		
Probabilistic reward task					♦		
Prediction error task							♦
Social cognition task			♦				
Other	Face categorization task		Arterial spin labelling				

CAN-BIND = Canadian Biomarker Integration Network in Depression; MDD = major depressive disorder; NA = not applicable; rTMS = repetitive transcranial magnetic stimulation; SSRI = selective serotonin reuptake inhibitor; TBI = traumatic brain Injury.
*Overall, the 7 studies are projected to include approximately 980 patients and 305 controls, for a total of approximately 3000 T_1 scans.
†Approximately 600 patient T_1 scans, approximately 300 control T_1 scans.

Table 2: Detailed scan acquisition parameters for structural MRI sequences (part 1 of 2)

CAN-BIND site	Toronto Western/ Toronto General Hospital	Centre for Addiction and Mental Health	McMaster University	University of Calgary	University of British Columbia	Sunnybrook Health Sciences Centre	Queen's University	Saint Michael's Hospital
CAN-BIND project	CAN-BIND-1 CAN-BIND-2	CAN-BIND-1 CAN-BIND-2	CAN-BIND-1	CAN-BIND-1 CAN-BIND-3	CAN-BIND-1 CAN-BIND-2	CAN-BIND-3	CAN-BIND-1 CAN-BIND-4 CAN-BIND-9	CAN-BIND-5 CAN-BIND-10
Scanner model	GE 3.0 T Signa HDxt	GE 3.0 T Discovery MR750	GE 3.0 T Discovery MR750	GE 3.0 T Discovery MR750	Phillips 3.0 T Intera	Phillips 3.0 T Achieva	Siemens 3.0 T TrioTim	Siemens 3.0 T Skyra
Software version	HD16.0_ V02_1131.a	DV24.0_ R01_1344.a	DV25.0_R02_1549.b	DV25.0_R02_1549.b	3.2.3, 3.2.3.1	3.2.2, 3.2.2.0	syngo MR B19	syngo MR E11
Coil	GE 8HRBRAIN	GE 8HRBRAIN	GE 32Ch Head/ GE HNS Head	GE HNS Head	SENSE-Head-8	SENSE-Head-8	12-channel head matrix coil	20-channel head/neck coil
T_1-weighted scan, sagittal acquisition								
Repetition time, ms	7.5[a]	6.4[b]	6.4[b]	6.4[b]	6.57	6.50	1760[c]	1840
Echo time, ms	2.86[d]	2.8[e]	2.8[e]	2.8[e]	2.9[f]	3.0	2.2[g]	3.4
Inversion time, ms	450	450	450	450	950	950	950[h]	950
Flip angle, degrees	15	15	15	15	8	8	15	15
Pixel bandwidth	260[i]	260[i]	260[j]	260[i]	241[k]	241	199	200
Matrix dimension, pixels	240 × 240[l]	240 × 240[l]	240 × 240[l]	240 × 240[l]	240 × 240[m]	240 × 240	256 × 256	256 × 256
Voxel dimension, mm	1 × 1 × 1	1 × 1 × 1	1 × 1 × 1	1 × 1 × 1	1 × 1 × 1	1 × 1 × 1	1 × 1 × 1	1 × 1 × 1
Slices, *n*	176	180[n]	180[n]	180[n]	180[o]	155	192	176
Acquisition times, min	03:40	03:30	03:30	03:30	09:50	09:53	04:06	07:53
Diffusion tensor imaging								
Repetition time, ms	8000[p]	8000[p]	8000[p]	8000[p]	9000[p]	8999	8000[p]	8200
Echo time, ms	94[q]	94[q]	94[q]	94[q]	94[q]	94	94[q]	94
Flip angle, degrees	90	90	90	90	90	90	90	90
Pixel bandwidth	5208[r]	5208[r]	5208	5208[s]	3326[t]	3256	2894[u]	1410
Matrix dimension, pixels	96 × 96	96 × 96	96 × 96	96 × 96	96 × 96	96 × 96	96 × 96	96 × 96
Voxel dimension, mm	2.5 × 2.5 × 2.5	2.5 × 2.5 × 2.5	2.5 × 2.5 × 2.5	2.5 × 2.5 × 2.5[v]	2.5 × 2.5 × 2.5[w]	2.4 × 2.4 × 2.4	2.5 × 2.5 × 2.5	2.5 × 2.5 × 2.5
Diffusion directions, *n*	31	31	31	31	30	32	30	30
Diffusion *b* value	1000	1000	1000	1000 (CAN-BIND-1); 1000 and 2500 (CAN-BIND-3)	1000	1000 and 2500	1000	1000
Diffusion images with $b = 0$	6	6	6	6	6	6	6	6
Acquisition times, min	05:04	05:04	05:04	5:04 (CAN-BIND-1); 7:12 and 7:12 (CAN-BIND-3)	04:57	5:15 and 5:15	04:34	04:40

Table 2: Detailed scan acquisition parameters for structural MRI sequences (part 2 of 2)

CAN-BIND site	Toronto Western/ Toronto General Hospital	Centre for Addiction and Mental Health	McMaster University	University of Calgary	University of British Columbia	Sunnybrook Health Sciences Centre	Queen's University	Saint Michael's Hospital
T_2-weighted proton density scan, axial acquisition								
Repetition time, ms	6583[x]	5724[y]	6004[z]	6004[aa]	5500	5428	11900[bb]	NA
Echo time 1, ms	7.3	7.5	7.5	7.5	16.8	16.8	8.1	NA
Echo time 2, ms	87.8[cc]	90.3	90.3	90.3	88.0	88.0	105.0	NA
Flip angle, degrees	90	125	125	125	125	125	125	NA
Pixel bandwidth	326	326	326	326	188	188	326	NA
Matrix dimension, pixels	192 × 192	192 × 192	192 × 192	192 × 192	192 × 192	192 × 138	192 × 168	NA
Voxel dimension, mm	1.25 × 1.25 × 2.5	1.25 × 1.25 × 2.5	1.25 × 1.25 × 2.5	1.25 × 1.25 × 2.5	1.25 × 1.25 × 2.5	1.25 × 1.37 × 2.5	1.25 × 1.25 × 2.5	NA
Slices, *n*	116	116	116	116	116	116	116	NA
Acquisition times, min	01:47	01:32	01:27	01:30	04:35	02:23	01:47	NA

CAN-BIND = Canadian Biomarker Integration Network in Depression; NA = not applicable.
[a]For *n* = 42, the repetition time for GE Signa was 7.2 ms.
[b]For *n* = 59, the repetition time for GE Discovery ranged from 7.2 ms to 7.7 ms.
[c]For *n* = 11, the repetition time for Siemens was 1900 ms.
[d]For *n* = 42, the echo time for GE Signa was 2.7 ms.
[e]For *n* = 59, the echo time for GE Discovery ranged from 2.7 ms to 2.9 ms.
[f]For *n* = 27, the echo time for Philips Achieva was 3.6 ms.
[g]For *n* = 11, the echo time for Siemens was 2.7 ms.
[h]For *n* = 11, the inversion time for Siemens was 900 ms.
[i]For *n* = 78, the pixel bandwidth for GE was 244.
[j]For *n* = 23, the pixel bandwidth for GE was 122.
[k]For *n* = 27, the pixel bandwidth for Philips was 191.
[l]For *n* = 91, the matrix dimensions for GE were 220 × 220.
[m]For *n* = 27, the matrix dimensions for Phillips were 256 × 256.
[n]For *n* = 49, the number of slices for GE Discovery was 176.
[o]For *n* = 27, the number of slices for Philips was 170.
[p]For *n* = 139, the repetition time was 14000 ms. The repetition time for diffusion tensor imaging was adjusted to be consistent (reduced to 8000 ms for GE scanners and 8999/9000 ms for Philips scanners) early in CAN-BIND-1. Subsequent CAN-BIND studies used the reduced repetition time.
[q]For *n* = 145, the echo time for diffusion tensor imaging sequences ranged from 78 to 85 ms.
[r]For *n* = 49, the pixel bandwidth for GE was 3906.
[s]For *n* = 19, the pixel bandwidth was 1953.
[t]For *n* = 27, the pixel bandwidth was 3256.
[u]For *n* = 11, the pixel bandwidth was 1408.
[v]For *n* = 19, the voxel dimensions was 0.9 × 0.9 × 2.5.
[w]For *n* = 27, the voxel dimension was 2.4 × 2.4 × 2.4.
[x]For *n* = 42, the repetition time was 7167 ms.
[y]For *n* = 7, the repetition time was 5794 ms.
[z]For *n* = 23, the repetition time was 5921 ms.
[aa]For *n* = 19, the repetition time was 6064 ms.
[bb]For *n* = 11, the repetition time was 11670 ms.
[cc]For *n* = 42, the echo time was 88.32 ms.

white-matter integrity; and resting-state and task-based blood-oxygenation-level-dependent fMRI sequences to assess functional networks and pathways. The CAN-BIND-3 study also uses arterial spin labelling to measure cerebral blood flow. Protocols have been informed by a review of the relevant literature, consultation with other experts in the field and group consensus, taking into account each scanner's capabilities.

Six scanner models are used across the clinical sites, mandating extensive and ongoing quality-control processes:[21] a Discovery MR750 3.0 T (GE Healthcare), a Signa HDxt 3.0 T (GE Healthcare), a MAGNETOM Trio (Siemens Healthcare), a MAGNETOM Skyra (Siemens Healthcare), an Achieva 3.0 T (Philips Healthcare) and an Intera 3.0 T (Philips Healthcare).

Stimulus sizes, instructions to participants and support materials are standardized across sites. All behavioural data are captured using E-Prime version 2.0 Professional (Psychology Software Tools). For CAN-BIND-5 and CAN-BIND-10, PsychoPy,[27] Inquisit (Millisecond) and Presentation (www.neurobs.com/) are also used. Guidelines and practices have been established for instructing participants to remain still throughout the scan, for applying a fiducial marker on the right temple, and for collecting respiratory bellows and peripheral gating (pulse oximetry) data using standard instruments provided by each manufacturer.

Whole-brain T_1-weighted structural scan

Whole-brain T_1-weighted structural scans are noninvasive, readily acquired and, because they are relatively short, generally well tolerated; these are features that may be important for identifying a potential biomarker.[28] Structural MRI studies in patients with MDD have revealed widespread corticolimbic differences in grey matter[29,30] and white matter,[31] suggesting that there are detectable alterations in the structure of key brain regions that could inform clinically relevant outcomes. Studies examining how well structural MRI data may be able to diagnose depression report accuracy rates of 48% to 91%.[32–37] Some studies have reported that structural alterations predict outcomes of treatment at the group level.[38–46]

The T_1-weighted scans are acquired with a 3D isotropic resolution of 1 mm. For further detail on whole-brain T_1-weighted imaging parameters, see Table 2. Information to confirm participant orientation is collected by placing a small vitamin E capsule on the right temple as a stereotactic marker (https://adni.loni.usc.edu/wp-content/uploads/2010/09/ADNI_MRI_Tech_Proc_Manual.pdf). Further information is included in Setup and Quality Assurance of MRI Protocols.

Whole-brain DTI

Diffusion tensor imaging studies have demonstrated altered white-matter microstructural abnormalities in patients with MDD. Decreased fractional anisotropy, a proxy measure of the directionality of diffusion, has been reported in patients with MDD in the frontal and occipital (fusiform) regions.[47–50] Fibre tracking has revealed the involvement of similar structures in MDD.[47] White-matter alterations have predicted treatment outcomes with up to 65% accuracy.[33,37] In another study, elevated baseline fractional anisotropy in tracts connecting to the right amygdala has been associated with remission following SSRI treatment.[51]

The CAN-BIND DTI acquisition protocol employs a single-shot, spin-echo, echo planar imaging sequence with diffusion sensitizing gradients applied in 31 noncollinear directions (b = 1000 s/mm^2) and 6 volumes with b = 0 s/mm^2. For CAN-BIND-3, diffusion sensitizing gradients were applied in 45 noncollinear directions, with 8 images collected at b = 1000 s/mm^2 and 8 images collected at b = 2500 s/mm^2. Increasing the number of diffusion-encoded directions improves the accuracy and/or robustness of diffusion tensor estimation,[52] and having more directions allows for the removal of any corrupted directions (e.g., due to motion/movement).[53] See Table 2 for further details on the parameters for whole-brain DTI.

Resting-state fMRI

Resting-state fMRI allows for the identification of task-independent and spontaneous neural activation that coincides temporally to form neural networks[54] such as the default mode network (e.g., see Greicius and colleagues[55]), the salience network or cognitive control network (e.g., Menon,[56] Menon and Uddin,[57] or Seeley and colleagues[58]), and the affective network.[59–63] The default mode network shows abnormal patterns of functional connectivity in MDD[55,64–66] that may normalize following treatment[67,68] or may be associated with treatment resistance.[69]

Resting-state data are collected over a 10-minute scan during which participants are instructed to lie still, keep their eyes open and focus on a fixation cross.[70] Standardized instructions are used across sites. Images are obtained using a whole-brain T_2*-sensitive blood-oxygen-level-dependent echo planar imaging series, with a repetition time of 2000 ms, an echo time of 30 ms and voxel dimensions of 4 mm × 4 mm × 4 mm, kept constant across sites and scanners. See Table 3 for further details on the parameters for resting-state fMRI.

Task-based fMRI

Task-based fMRI studies suggest that there may be different patterns of change associated with specific treatments or classes of treatment.[68,71–76] The CAN-BIND substudies test treatment- and population-specific questions, using cognitive-functional tasks that are described in detail in Appendix 1.

Task-relevant instructions are standardized and given before the scan sessions. Each site uses a comparable, custom-manufactured, magnet-compatible input device (www.mrn.org/collaborate/imaging-equipment) to record participants' responses. Acquisition parameters are similar to those for resting-state fMRI, and are listed in detail in Appendix 1, Table S1 and Table S2.

Arterial spin labelling

Arterial spin labelling perfusion MRI measures regional cerebral blood flow and may be used to study subtle brain

perfusion changes in psychiatric illnesses. Perfusion patterns may hold promise as objective biomarkers for tracking illness progression, as well as pharmacological/treatment effects in various neuropsychiatric disorders.[77]

Data storage

Clinical data are collected and stored in the Ontario Brain Institute's Centre for Ontario Data Exploration (Brain-CODE; www.braincode.ca/; Vaccarino and colleagues[78]). This online neuroinformatics platform allows researchers to collaborate across distances and work efficiently at multiple sites. Brain-CODE is deployed at the Centre for Advanced Computing at Queen's University in Kingston, Ontario. The Centre for Advanced Computing is a member of the Compute Canada high-performance computing consortium, which supports regulatory-compliant processes for securing the privacy of health care data (https://cac.queensu.ca/overview). Online clinical and neuroimaging data are accessed on secure websites via restricted portals that require unique usernames and passwords for each member of the study team. User profiles are assigned only to study personnel who require access to enter and verify data, and credentials for each user are vetted by the program manager.

The SPReD database (originally the Stroke Patient Recovery Research Database) is a comprehensive online repository powered by the open-source Extensible Neuroimaging Archiving Toolkit (XNAT) imaging informatics platform,[79,80] where neuroimaging data are uploaded and stored. Structural and functional MRI data are uploaded from each site as Digital Imaging and Communications in Medicine (DICOM) images. Supplementary records, such as behavioural and physiological data, and session notes associated with an imaging session, are uploaded through a special subprocess.

Neuroinformatics framework

The CAN-BIND neuroinformatics framework consists of software, tools, pipelines and procedures designed to ensure high-quality data acquisition, databasing, archiving, assessment, analysis and tracking, an overview of which is shown in Figure 1. The primary platform for this set of tools is XNAT/SPReD, provided through Brain-CODE. In addition to the MRI data being captured and managed through XNAT/SPReD, other study-related data are captured using OpenClinica and RedCap. A visualization "dashboard" built using SpotFire (http://spotfire.tibco.com/) is used to upload aggregated data tracking and analytics results from phantom data (see Fig. 2 and Fig. 3).

CAN-BIND quality control and quality assurance procedures

The importance of quality assurance and control in multisite studies is recognized.[81] The full spectrum of data quality control and data quality assurance methods was implemented early in CAN-BIND-1. These methods are described in the sections that follow and have been applied to most of the CAN-BIND substudies. The CAN-BIND-2 and CAN-BIND-3 studies have not been uploading their data to SPReD, so the automated adherence checks described here do not apply to them.

Quality control

Data file-naming convention and adherence checks

Participants are assigned unique identification codes, which are standardized to contain a program code (3 letters), a study number (2 digits), a site identification code (3 letters) and a participant number (4 digits; e.g., CBN01_UCA_0001). These file-naming conventions are applied to MRI and behavioural data files. A pipeline assessing the consistency of naming conventions is implemented in XNAT/SPReD; if noncompliance is detected, notification is sent to relevant study personnel asking them to implement corrections, with

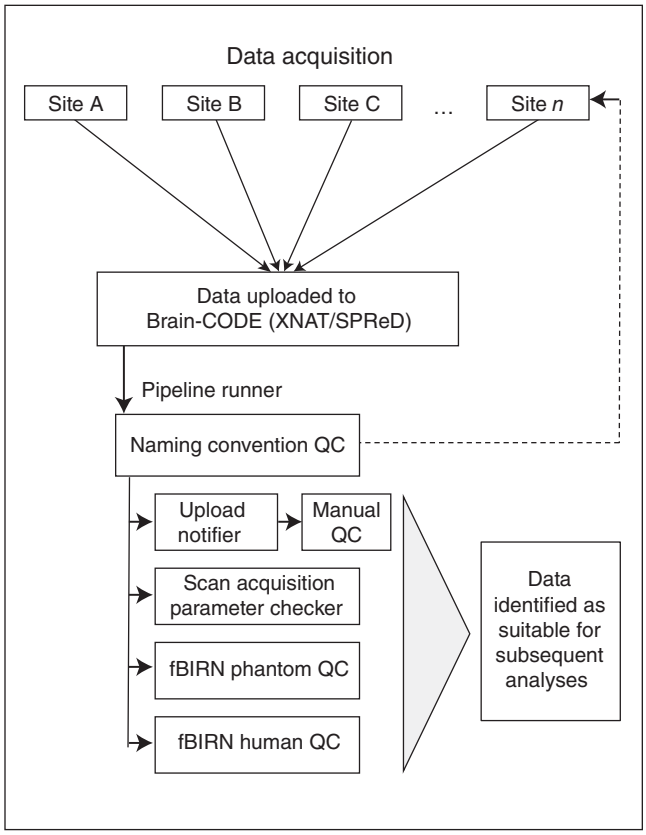

Fig. 1: Overview of the CAN-BIND neuroinformatics framework. Data from each site is uploaded to Brain-CODE, where specifically designed pipelines check the data for compliance with scan acquisition parameters, naming convention and completeness. Automatic messages are sent to initiate manual QC. The CAN-BIND neuroinformatics framework also includes pipelines for the analysis of phantom data. CAN-BIND = Canadian Biomarker Integration Network in Depression; fBIRN = Functional Biomedical Informatics Research Network; QC = quality control; SPReD = originally named the Stroke Patient Recovery Research Database; XNAT = Extensible Neuroimaging Archiving Toolkit.

follow-up until corrections are performed. The data will not undergo subsequent quality-control checks until file-naming conventions have been adhered to.

Parameter adherence checks of MRI protocols

Also implemented in SPReD is a quality-control pipeline for MRI protocols, which compares the acquisition parameters of newly uploaded scans against a reference protocol. Reference protocols have been established for each site and scanner type, taking into account the fact that scan parameters are necessarily different among scanners and manufacturers. The reference protocol defines the sequences and appropriate acquisition parameters (values) for each sequence. If discrepancies are identified between the data uploaded and the reference protocol, e-mail notifications are sent to study personnel, asking them to identify causes for adherence check failures and pointing to the need for possible rescanning.

Image quality

It is necessary to obtain images of sufficient subjective quality, free of motion artifacts, covering a full field of view and free of other scanner-related artifacts in order to process the data through various pipelines. Certain sequences, such as resting-state fMRI, are more susceptible to motion and other artifacts. Others, such as T_1-weighted images, are of such paramount importance that tolerance for motion or other

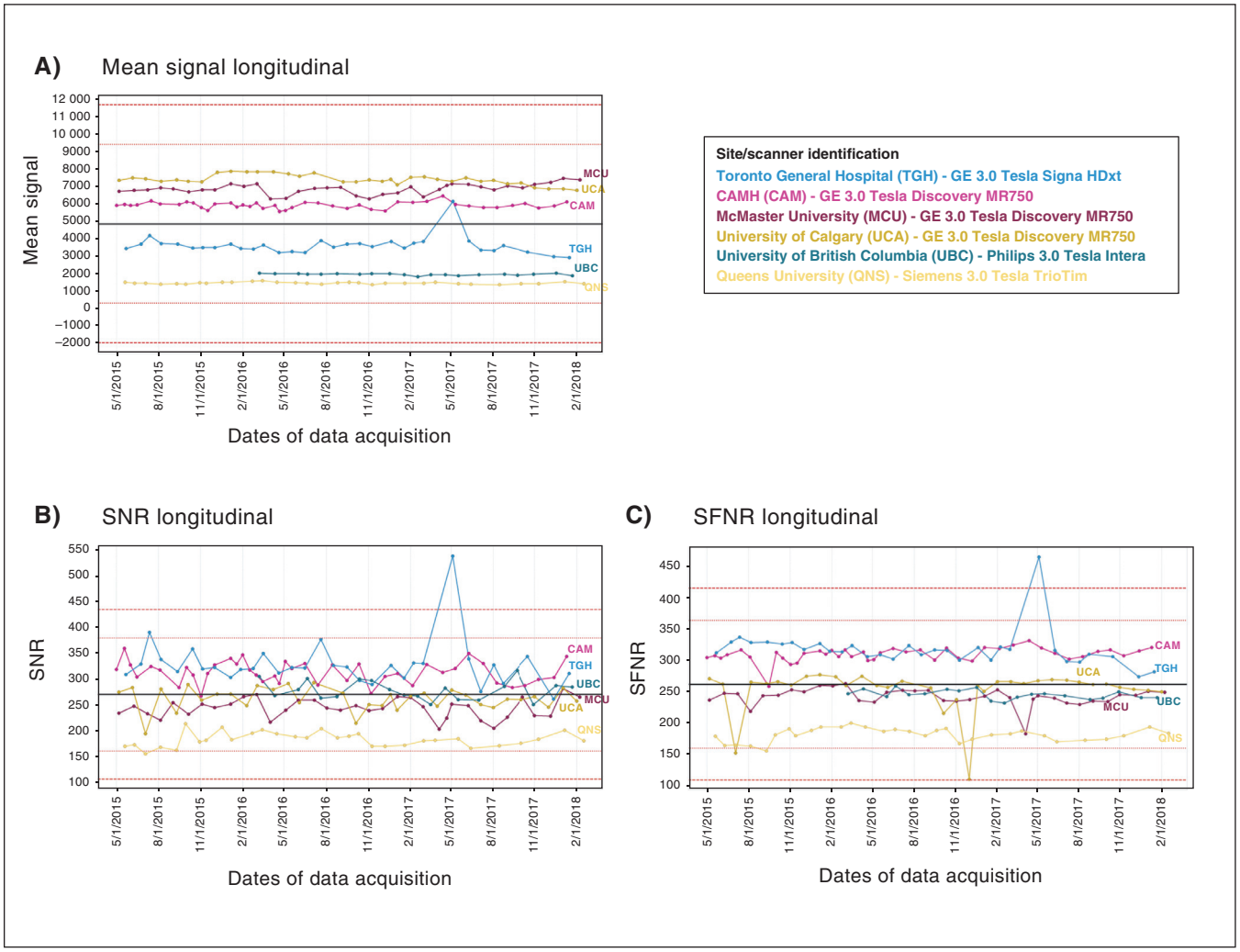

Fig. 2: Examples of data quality tracking and assessment pipelines. Phantom data are tracked longitudinally to monitor adherence and data quality of imaging protocols. Illustrated here is an example where spiking in the overall mean signal intensity across acquired images at one data acquisition site (light blue) was tracked to be related to its SNR and its SNFR. (A) Mean signal longitudinal: this metric tracks the average overall signal intensity across all voxels and images, per scanning session. (B) SNR longitudinal: this metric tracks the average overall SNR. The mean SNR is the static spatial noise × image across a 21 × 21 voxel region of interest centred on the image. The signal summary value is the average of the signal image across this same region of interest. Then, SNR = (signal summary value)/√(variance summary value/number of time points). (C) SFNR longitudinal: the SFNR is the voxel-wise ratio of the temporal variance standard deviation and temporal mean intensity of the 4-dimensional phantom image after quadratic detrending. The SFNR summary value is the mean SFNR value within the evaluation region of interest (a 21 × 21 voxel region in the centre of the image). SFNR = signal-to-fluctuation-noise ratio; SNR = signal-to-noise ratio.

artifacts is low because they influence the quality of the data and the usability of other sequences, which are typically coregistered to T_1-weighted scans. Trained expert quality-control raters are automatically notified when new data are uploaded to SPReD. They perform visual assessment of the MRI data image quality using the SPReD interface. The quality-control raters have received training via ONDRI, based on the data quality control protocol from the Centre for Brain Science at Harvard University.[82] Raters compare their assessments and comments on scan quality for subsets of data collected at participating CAN-BIND sites. Each imaging sequence is reviewed independently for quality, including full-brain coverage (on a 2-point scale: complete or incomplete), motion and other image artifacts (on a 3-point scale: none, mild or severe), based on the data quality-control protocol.[82] Imaging that has insufficient coverage, excessive motion as identified by visual inspection of rigid uniform stripes running horizontally across the brain[82] or other imaging artifacts that may interfere with future processing and usability are marked as questionable or unusable, depending on severity. If images are flagged as unusable, they are unavailable for subsequent analysis, and a request is made to the study site to rescan the participant whenever feasible. An upload delay dashboard also serves to inform program managers of the delay time in uploading data once it has been acquired.

Assessment of site differences

Cross-site T_1 piloting included a travelling participant or "human phantom," who travelled to each CAN-BIND-1 site for anatomic scans to document within and between-site variance.

Setup and quality assurance of MRI protocols

Setup of scan parameters

Prior to study launch, scan parameters from DICOM header files were examined to match scan parameters

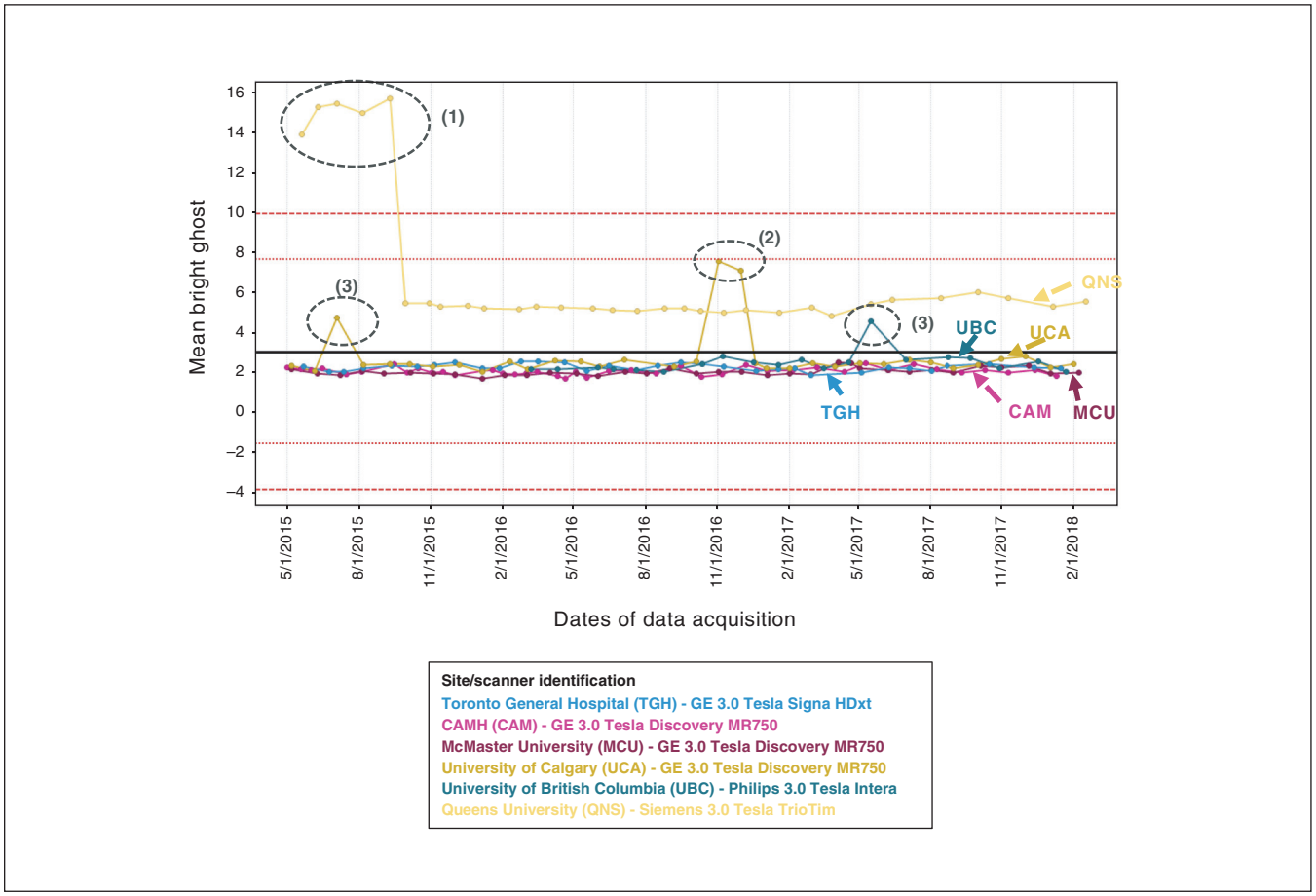

Fig. 3: Examples of data quality tracking and assessment pipelines. Phantom data are tracked longitudinally to monitor adherence and data quality of imaging protocols. Illustrated here are examples where the mean intensity of ghost-only voxels showed deviations; investigation and explanation of these anomalies are listed in 1, 2 and 3, below. Mean bright ghost longitudinal: ghost metrics are calculated for each volume by taking a dilated mask ("original mask") of the data, and shifting it by N/2 voxels in the appropriate axis to create a "ghost mask." Whereas the mean intensities of those voxels in the ghost mask and not in the original mask is the "mean ghost" value, the "mean bright ghost" is the mean intensity of the top 10% of ghost-only voxels. (1) Anomaly: investigation led to protocol adjustments. (2) Receiver coil failure: addressing failure resulted in data returning to the level seen previously. (3) Anomalies, investigation: corresponding human functional MRI scans acquired around this date appeared fine; subsequent phantom scans were fine.

Table 3: Detailed scan acquisition parameters for resting-state functional MRI sequences

CAN-BIND site	Toronto Western/ Toronto General Hospital	Centre for Addiction and Mental Health	McMaster University	University of Calgary	University of British Columbia	Sunnybrook Health Sciences Centre	Queen's University	Saint Michael's Hospital
CAN-BIND project	CAN-BIND-1 CAN-BIND-2	CAN-BIND-1 CAN-BIND-2	CAN-BIND-1	CAN-BIND-1 CAN-BIND-3	CAN-BIND-1 CAN-BIND-2	CAN-BIND-3	CAN-BIND-1 CAN-BIND-4 CAN-BIND-9	CAN-BIND-5 CAN-BIND-10
Scanner model	GE 3.0 T Signa HDxt	GE 3.0 T Discovery MR750	GE 3.0 T Discovery MR750	GE 3.0 T Discovery MR750	Phillips 3.0 T Intera	Phillips 3.0 T Achieva	Siemens 3.0 T TrioTim	Siemens 3.0 T Skyra
Software version	HD16.0_ V02_1131.a	DV24.0_ R01_1344.a	DV25.0_ R02_1549.b	DV25.0_ R02_1549.b	3.2.3, 3.2.3.1	3.2.2, 3.2.2.0	syngo MR B19	syngo MR E11
Coil	GE 8HRBRAIN	GE 8HRBRAIN	GE 32Ch Head/ GE HNS Head	GE HNS Head	SENSE-Head-8	SENSE-Head-8	12-channel head matrix coil	20-channel head/ neck coil
Resting-state functional MRI								
Repetition time, ms	2000.0	2000.0	2000.0	2000.0	2000.0	2000.0	2000.0	2000.0
Echo time, ms	30.0	30.0	30.0	30.0	30.0	30.0	30.0*	30.0
Field of view	256	256	256	256	256	256	1536 (mosaic)	256
Flip angle, degrees	75.00	75.00	75.00	75.00	75.00†	75.00	75.00	75.00
Pixel bandwidth	7812.5	7812.5	7812.5	7812.5	4807.0	3589.0	2232.0	3395.0
Matrix dimension, pixels	64 × 64	64 × 64	64 × 64	64 × 64	64 × 64	64 × 64	64 × 64	64 × 64
Voxel dimension, mm	4 × 4 × 4	4 × 4 × 4	4 × 4 × 4	4 × 4 × 4	4 × 4 × 4	4 × 4 × 4	4 × 4 × 4	4 × 4 × 4
Volumes, *n*	300	300	300	300	300	300	300	300
Slices, *n*	34‡	36§	36	36	36	40	36¶	37
Acquisition times, min	10:00	10:00	10:00	10:00	10:06	10:06	10:00	10:08

CAN-BIND = Canadian Biomarker Integration Network in Depression.
*For n = 11, echo time = 25.0 ms.
†For n = 27, flip angle = 90 degrees.
‡For n = 40, number of slices = 40.
§For n = 7, number of slices = 40.
¶For n = 11, number of slices = 40.

across CAN-BIND-1 sites to a majority consensus where possible (exceptions included receiver bandwidth of multiple scans and acceleration type). Quality assurance test sample data were acquired from CAN-BIND-1 sites and examined; then, recommendations were made to each site if adjustments or revisions were required. Acquisition parameters were transferred digitally from sites with a GE Discovery 750, and by PDF from sites with other scanners. Technologists entered the values and subsequently checked the DICOM headers. Following revisions, this process was repeated. Next, a human phantom/expert visited the CAN-BIND-1 sites to identify scanning issues and acquire data. Subsequently, T_1 acquisitions at sites without GE Discovery 750 scanners were matched by acquiring multiple flip-angle/inversion time values and identifying those that gave a contrast-to-noise measure that was most similar to the GE Discovery 750 scanners. The T_1 scans were prescribed to a sagittal acquisition using a nonselective radiofrequency pulse; fMRI and DTI scans were acquired as true axial scans to reduce cross-site variation. In addition, fMRI and DTI scans were acquired using fat saturation at all sites, rather than having some sites use spectral–spatial pulses. Protocol corrections were made to ensure that image resampling after acquisition was not performed (rhimsize was set on GE scanners to prevent interpolation of images in DTI). Acquisition in DTI was shortened from a repetition time of 14 000 ms to one of 9000 ms. This reduced the scan time, while leaving contrast unaffected, because it maintained at least 6 T_1 time constants for both grey and white matter. Scan acquisition parameters according to site for structural MRI data — including 3-dimensional T_1-weighted scans, DTI scans and T_2-weighted proton density scans — are listed in Table 2, and parameters for functional MRI data are listed in Table 3 and Appendix 1, Table S1 and Table S2.

Monitoring and quality assurance of imaging parameters

Since the CAN-BIND launch, all CAN-BIND-1 sites have obtained monthly scans of 2 geometric phantoms (a spherical agar phantom developed by the fBIRN consortium, and a custom-built cylindrical model using plastic LEGO blocks)[20,83] to facilitate scanner calibration and troubleshooting over the long term. Examples of the longitudinal tracking of phantom data quality are illustrated in Figure 2 and Figure 3. Phantom scans are also acquired at St. Michael's Hospital for CAN-BIND-5 and CAN-BIND-10. Phantom scans are not collected at

Sunnybrook Health Sciences Centre, the second data acquisition site for CAN-BIND-3.

Setup of fMRI paradigms

To standardize the viewing angle for fMRI task stimuli, a standard grid was displayed at each site, viewing distance was measured, and the visual angle of the projected image was calculated. Consistent cross-site viewing angle was established using specific display parameters in the E-Prime software for each site. Across sites, the version of the E-Prime stimulus display software was matched. Button responses and ASCII key codes were confirmed and used in site-specific E-Prime task versions. Data files produced by each paradigm were examined to confirm that the proper response information was being acquired and logged.

Sites were also provided with a scripted set of instructions to be issued before resting-state scans, as well as a standardized fixation cross for participants to focus on during the resting state scan. A set of participant orientation/training slides were instituted for functional tasks. Randomization schedules were provided for the functional task version administered (e.g., A/B/C for the go/no-go task) and task order between, for example, go/no-go and reward tasks. For detail on fMRI tasks, see Appendix 1. Study coordinators were provided with a guide to follow when checking the fidelity of the acquired behavioural data. Finally, conference calls were held with the research coordinators at each site to ensure that standard operating procedures were communicated and instituted.

Discussion

The neuroinformatics procedures and pipelines employed in CAN-BIND address many challenges associated with combining MRI data from multisite studies. Considerable effort has been focused on the image acquisition protocols, and procedures have been implemented — automated, where possible — to ensure the ongoing quality of the images. We recognize, however, that residual differences in neuroimaging data collected across different sites and MRI vendors will likely still exist.

The "reproducibility in science crisis"[84] has required that imaging studies examine common approaches to study design, monitoring and interpretation. Issues underlying the difficulty with replication are multifaceted, and protocols are emerging to ensure that imaging studies are well planned, well executed and well reported. This includes making the details of how studies are designed, executed and analyzed more apparent and transparent.[85,86] This paper aims to provide methodological detail for the CAN-BIND studies in a transparent and comprehensive manner. As evident from Figure 1, there are common data elements across the CAN-BIND program substudies, specifically for 3D anatomic scans, resting-state fMRI and DTI. Scan parameters (as detailed in Table 2 and Table 3) are as comparable and compatible as scanner manufacturer and type allow. Quality-control procedures, such as checking protocol adherence for participant scans and manual quality control of acquired data, are performed for most substudies, based on an agreed-upon protocol. For example, although CAN-BIND-2 and CAN-BIND-3 are not currently uploading data to SPReD for automatic protocol adherence checks, data are being manually inspected for data quality.

Limitations

Although we consider it a strength that the CAN-BIND protocol is applied across participants with a wide age range (12 to 70 years), age-related differences will need to be assessed with caution, as will differences in sex and other demographic factors. We did not assess for the presence of cerebrovascular disease in our sample, although there is an association between cardiovascular disease and MDD,[87] but also with MDD and other medical conditions.[88] Given the relatively young age of our samples (e.g., Lam and colleagues,[19] Addington and colleagues,[24] Santesteban-Echarri and colleages[89] and Kennedy and colleagues[90]), this is unlikely to be a driving factor in neuroimaging results, but medical comorbidity is an important consideration in studies of psychiatric disease. No routine screening for substance use was performed, potentially affecting our findings. As noted above, CAN-BIND-2 and CAN-BIND-3 are not subject to the automatic adherence checks that would result from uploading to SPReD.

Conclusion

The CAN-BIND program is unusual in that it uses a suite of common imaging protocols across a variety of studies that examine predictive markers of response to various treatment modalities in MDD. Although each CAN-BIND substudy is expected to yield valuable information, the consistent protocols, centralized data collection and quality control that will eventually allow for cross-study investigations is likely to be the greatest strength of CAN-BIND.

Deidentified CAN-BIND data eventually will be shared by the Ontario Brain Institute with other collaborators and third parties for research purposes.[91] These data sets may inform clinical research teams with similar data sets comparing MDD with other psychiatric conditions, or comparing different treatment modalities. Thus, rigorous, recorded quality control of CAN-BIND neuroimaging and related data are crucial for ensuring the value of this data set to the greatest number of investigators. When fully realized, the CAN-BIND data set will provide a comprehensive resource for researchers interested in predictors, moderators and mediators of response to treatment in MDD.

Acknowledgements: CAN-BIND is an Integrated Discovery Program carried out in partnership with, and with financial support from, the Ontario Brain Institute, an independent nonprofit corporation funded partially by the Ontario government. The opinions, results and conclusions are those of the authors, and no endorsement by the Ontario Brain Institute is intended or should be inferred. Additional funding is provided by the Canadian Institutes of Health Research, Lundbeck, Bristol-Myers Squibb and Servier. Funding and/or in-kind support is also provided by the investigators' universities and academic institutions. All study medications are independently purchased at wholesale market values.

Affiliations: From the Department of Psychiatry, Cumming School of Medicine, University of Calgary, Calgary, Alta., Canada

(MacQueen, Hassel, Addington, Sharma); the Rotman Research Institute, Baycrest, and Department of Medical Biophysics, University of Toronto, Toronto, Ont., Canada (Arnott, Zamyadi, Strother); the Department of Psychology, Queen's University, Kingston, Ont., Canada (Bowie, Harkness, Milev); the Department of Radiology, University of Calgary, Calgary, Alta., Canada (Bray, Lebel); the Alberta Children's Hospital Research Institute, Calgary, Alta., Canada (Bray, Lebel); the Child and Adolescent Imaging Research (CAIR) Program, Calgary, Alta., Canada (Bray, Lebel); the Department of Psychology, Neuroscience and Behaviour, McMaster University, and St. Joseph's Healthcare Hamilton, Hamilton, Ont., Canada (Hall); the Krembil Research Institute and Centre for Mental Health, University Health Network, Toronto, Ont., Canada (Downar); the Institute of Medical Science, Faculty of Medicine, University of Toronto, Toronto, Ont., Canada (Downar); the Department of Psychiatry, Faculty of Medicine, University of Toronto, Toronto, Ont., Canada (Downar, Müller, Rizvi, Rotzinger, Kennedy); the Department of Psychiatry, Krembil Research Centre, University Health Network, University of Toronto, Toronto, Ont., Canada (Foster, Rotzinger, Kennedy); the Department of Psychiatry and Behavioural Neurosciences, McMaster University, and St. Joseph's Healthcare Hamilton, Hamilton, Ont., Canada (Foster, Frey); the Centre for Youth Bipolar Disorder, Sunnybrook Health Sciences Centre, Toronto, Ont., Canada (Goldstein); the Departments of Psychiatry and Pharmacology, Faculty of Medicine, University of Toronto, Toronto, Ont., Canada (Goldstein); the Department of Computer Science, University of Alberta, Edmonton, Alta., Canada (Harris); the University of British Columbia and Vancouver Coastal Health Authority, Vancouver, B.C., Canada (Lam, Vila-Rodriguez); the Department of Psychiatry, Queen's University and Providence Care Hospital, Kingston, Ont., Canada (Milev, Soares); the Campbell Family Mental Health Research Institute, Centre for Addiction and Mental Health, Toronto, Ont., Canada (Müller); the Department of Psychiatry, University of Michigan, Ann Arbor, MI, USA (Parikh); the Arthur Sommer Rotenberg Suicide and Depression Studies Program, Li Ka Shing Knowledge Institute and St. Michael's Hospital, Toronto, Ont., Canada (Rizvi); the Institute of Medical Science, Faculty of Medicine, University of Toronto, Toronto, Ont., Canada (Rizvi); the Department of Psychiatry, St. Michael's Hospital, University of Toronto, Toronto, Ont., Canada (Rotzinger, Soares, Yu); McGill University, Montréal, Que., Canada (Turecki); the Douglas Mental Health University Institute, Frank B. Common, Montréal, Que., Canada (Turecki); and the Keenan Research Centre for Biomedical Science, Li Ka Shing Knowledge Institute, St. Michael's Hospital, Toronto, Ont., Canada (Kennedy).

Competing interests: G. MacQueen reports consultancy/speaker fees from Lundbeck, Pfizer, Johnson & Johnson and Janssen, outside the submitted work. B. Frey reports grants and personal fees from Pfizer and personal fees from Sunovion, outside the submitted work. R. Milev reports grants, nonfinancial support and honoraria from Lundbeck, Janssen and Pfizer; personal fees and honoraria from Sunovion, Shire, Allergan and Otsuka; grants from Boehringer Ingelheim; and grants from the Ontario Brain Institute, the Canadian Institutes for Health Research and CAN-BIND, outside the submitted work. F. Vila-Rodriguez reports nonfinancial support from Magventure during the conduct of the study; grants from the Canadian Institutes for Health Research, Brain Canada, the Michael Smith Foundation for Health Research, and the Vancouver Coastal Health Research Institute; and personal fees from Janssen, outside the submitted work. S. Rizvi reports grants from Pfizer Canada, outside the submitted work. S. Strother reports grants from Canadian Biomarker Integration Network in Depression during the conduct of the study and grants from Ontario Brain Institute, outside the submitted work. He is also the chief scientific officer of the neuroimaging data analysis company ADMdx, Inc (www. admdx.com), which specializes in brain image analysis to enable diagnosis, prognosis and drug effect detection for Alzheimer disease and various other forms of dementia. R. Lam reports grants from Canadian Institutes of Health Research during the conduct of the study; grants from Asia-Pacific Economic Cooperation, VGH-UBCH Foundation, BC LEading Edge Endowment Fund, Janssen, Lundbeck, Pfizer and St. Jude Medical, outside the submitted work; personal fees from Allergan, Akili, CME Institute, Canadian Network for Mood and Anxiety Treatments, Janssen, Lundbeck, Lundbeck Institute, Pfizer, Otsuka, Medscape and Hansoh, outside the submitted work; travel expenses from Asia-Pacific Economic Cooperation outside the submitted work; and stock options from Mind Mental Health Technologies.

Contributors: G. MacQueen, S. Hassel, J. Addington, C. Bowie, S. Bray, J. Downar, J. Foster, B. Frey, B. Goldstein, K. Harkness, C. Lebel, R. Milev, D. Müller, S. Parikh, S. Rizvi, S. Rotzinger, C. Soares, S. Strother and S. Kennedy conceived and designed the article. R. Lam acquired the data. S. Hassel, S. Arnott, A. Davis, J. Harris, G. Sharma, J. Yu, M. Zamyadi and S. Strother analyzed and interpreted the data. G. MacQueen and S. Hassel wrote the article, which all authors reviewed. All authors approved the final version to be published and can certify that no other individuals not listed as authors have made substantial contributions to the paper.

Members of the CAN-BIND Investigator Team: www.canbind.ca/our-team

References

1. Ferrari AJ, Charlson FJ, Norman RE, et al. The epidemiological modelling of major depressive disorder: application for the Global Burden of Disease study 2010. *PLoS One* 2013;8:e69637.
2. Collins, PY, Patel V, Joestl SS, et al. Grand challenges in global mental health. *Nature* 2011;475:27-30.
3. American Psychiatric Association. *Diagnostic and statistical manual of mental disorders*. 5th ed. Washington (DC): APA; 2013.
4. Jack CR, Bernstein MA, Fox NC, et al. The Alzheimer's Disease Neuroimaging Initiative (ADNI): MRI methods. *J Magn Reson Imaging* 2008;27:685-91.
5. Fonseka TM, MacQueen GM, Kennedy SH. Neuroimaging biomarkers as predictors of treatment outcome in major depressive disorder. *J Affect Disord* 2017;233:21-35.
6. Keshavan A, Paul F, Beyer MK, et al. Power estimation for non-standardized multisite studies. *Neuroimage* 2016;134:281-94.
7. Thompson PM, Stein JL, Medland SE, et al. The ENIGMA Consortium: large-scale collaborative analyses of neuroimaging and genetic data. *Brain Imaging Behav* 2014;8:153-82.
8. Schmaal L, Veltman DJ, van Erp TGM, et al. Subcortical brain alterations in major depressive disorder: findings from the ENIGMA Major Depressive Disorder Working Group. *Mol Psychiatry* 2016;21:806-12.
9. Schmaal L, Hibar DP, Sämann PG, et al. Cortical abnormalities in adults and adolescents with major depression based on brain scans from 20 cohorts worldwide in the ENIGMA Major Depressive Disorder Working Group. *Mol Psychiatry* 2017;22:900-9.
10. Potkin SG, Ford JM. Widespread cortical dysfunction in schizophrenia: the fBIRN imaging consortium. *Schizophr Bull* 2009;35:15-8.
11. Weiner MW, Veitch DP, Aisen PS, et al. Alzheimer's Disease Neuroimaging Initiative. The Alzheimer's Disease Neuroimaging Initiative: a review of papers published since its inception. *Alzheimers Dement* 2012;8(Suppl):S1-68.
12. Gollub RL, Shoemaker JM, King MD, et al. The MCIC collection: a shared repository of multi-modal, multi-site brain image data from a clinical investigation of schizophrenia. *Neuroinformatics* 2013;11:367-88.
13. Shinohara RT, Oh J, Nair G, et al. Volumetric analysis from a harmonized multisite brain MRI study of a single subject with multiple sclerosis. *AJNR Am J Neuroradiol* 2017;38:1501-9.
14. Farhan SM, Bartha R, Black SE, et al. The Ontario Neurodegenerative Disease Research Initiative (ONDRI). *Can J Neurol Sci* 2017;44:196-202.
15. Williams LM, Rush AJ, Koslow SH, et al. International Study to Predict Optimized Treatment for Depression (iSPOT-D), a randomized clinical trial: rationale and protocol. *Trials*; 2011;12:4.
16. Grieve SM, Korgaonkar MS, Etkin A, et al. Brain imaging predictors and the international study to predict optimized treatment for depression: study protocol for a randomized controlled trial. *Trials* 2013;14:224.
17. Trivedi MH, McGrath PJ, Fava M, et al. Establishing moderators and biosignatures of antidepressant response in clinical care (EMBARC): rationale and design. *J Psychiatr Res* 2016;78:11-23.
18. Kennedy SH, Downar J, Evans KR, et al. The Canadian Biomarker Integration Network in Depression (CAN-BIND): advances in response prediction. *Curr Pharm Des* 2012;18:5976-89.

19. Lam RW, Milev R, Rotzinger S, et al. Discovering biomarkers for antidepressant response: protocol from the Canadian Biomarker Integration Network in Depression (CAN-BIND) and clinical characteristics of the first patient cohort. *BMC Psychiatry* 2016;16:105.
20. Friedman L, Glover GH. Report on a multicenter fMRI quality assurance protocol. *J Magn Reson Imaging* 2006;23:827-39.
21. Glover GH, Mueller BA, Turner JA, et al. Function biomedical informatics research network recommendations for prospective multicenter functional MRI studies. *J Magn Reson Imaging* 2012;36:39-54.
22. Jovicich J, Czanner S, Han X, et al. MRI-derived measurements of human subcortical, ventricular and intracranial brain volumes: reliability effects of scan sessions, acquisition sequences, data analyses, scanner upgrade, scanner vendors and field strengths. *Neuroimage* 2009;46:177-92.
23. Jovicich J, Marizzoni M, Sala-Llonch R, et al. PharmaCog Consortium. Brain morphometry reproducibility in multi-center 3T MRI studies: a comparison of cross-sectional and longitudinal segmentations. *Neuroimage* 2013;83:472-84.
24. Addington J, Goldstein BI, Wang JL, et al. Youth at-risk for serious mental illness: methods of the PROCAN Study. *BMC Psychiatry* 2018;18:219.
25. Hickie IB, Scott EM, Hermens DF, et al. Applying clinical staging to young people who present for mental health care. *Early Interv Psychiatry* 2013;7:31-43.
26. Blair JR, Spreen O. Predicting premorbid IQ: a revision of the national adult reading test. *Clin Neuropsychol* 1989;3:129-36.
27. Pierce JW. PsychoPy: psychophysics software in Python. *J Neurosci Methods* 2007;162:8-13.
28. Biomarkers Definitions Working Group. Biomarkers and surrogate endpoints: preferred definitions and conceptual framework. *Clin Pharmacol Ther* 2001;69:89-95.
29. Atkinson L, Sankar A, Adams TM, et al. Recent advances in neuroimaging of mood disorders: structural and functional neural correlates of depression, changes with therapy, and potential for clinical biomarkers. *Curr Treat Options Psychiatry* 2014;1:278-93.
30. Sankar A, Zhang T, Gaonkar B, et al. Diagnostic potential of structural neuroimaging for depression from a multi-ethnic community sample. *BJPsych Open* 2016;2:247-54.
31. Cole J, Chaddock CA, Farmer AE, et al. White matter abnormalities and illness severity in major depressive disorder. *Br J Psychiatry* 2012;201:33-9.
32. Costafreda SG, Chu C, Ashburner J, et al. Prognostic and diagnostic potential of the structural neuroanatomy of depression. *PLoS One* 2009;4:e6353.
33. Gong Q, Wu Q, Scarpazza C, et al. Prognostic prediction of therapeutic response in depression using high-field MR imaging. *Neuroimage* 2011;55:1497-503.
34. Liu F, Guo W, Yu D, et al. Classification of different therapeutic responses of major depressive disorder with multivariate pattern analysis method based on structural MR scans. *PloS One* 2012;7:e40968.
35. Mwangi B, Ebmeier KP, Matthews K, et al. Multi-centre diagnostic classification of individual structural neuroimaging scans from patients with major depressive disorder. *Brain* 2012;135:1508-21.
36. Serpa MH, Ou Y, Schaufelberger MS, et al. Neuroanatomical classification in a population-based sample of psychotic major depression and bipolar I disorder with 1 year of diagnostic stability. *BioMed Res Int* 2014;2014:706157.
37. Kambeitz J, Cabral C, Sacchet MD, et al. Detecting neuroimaging biomarkers for depression: a meta-analysis of multivariate pattern recognition studies. *Biol Psychiatry* 2017;82:330-8.
38. Frodl T, Jäger M, Smajstrlova I, et al. Effect of hippocampal and amygdala volumes on clinical outcomes in major depression: a 3-year prospective magnetic resonance imaging study. *J Psychiatry Neurosci* 2008;33:423-30.
39. Frodl T, Koutsouleris N, Bottlender R, et al. Reduced gray matter brain volumes are associated with variants of the serotonin transporter gene in major depression. *Mol Psychiatry* 2008;13:1093-101.
40. Frodl TS, Koutsouleris N, Bottlender R, et al. Depression-related variation in brain morphology over 3 years: effects of stress? *Arch Gen Psychiatry* 2008;65:1156-65.
41. Frodl T, Meisenzahl EM, Zetzsche T, et al. Hippocampal and amygdala changes in patients with major depressive disorder and healthy controls during a 1-year follow-up. *J Clin Psychiatry* 2004;65:492-9.
42. Frodl T, Meisenzahl EM, Zill P, et al. Reduced hippocampal volumes associated with the long variant of the serotonin transporter polymorphism in major depression. *Arch Gen Psychiatry* 2004;61:177-83.
43. Meisenzahl EM, Koutsouleris N, Bottlender R, et al. Structural brain alterations at different stages of schizophrenia: a voxel-based morphometric study. *Schizophr Res* 2008;104:44-60.
44. Fu CHY, Costafreda SG, Sankar A, et al. Multimodal functional and structural neuroimaging investigation of major depressive disorder following treatment with duloxetine. *BMC Psychiatry* 2015;15:82.
45. Fu CHY, Steiner H, Costafreda SG. Predictive neural biomarkers of clinical response in depression: a meta-analysis of functional and structural neuroimaging studies of pharmacological and psychological therapies. *Neurobiol Dis* 2013;52:75-83.
46. Vakili K, Pillay SS, Lafer B, et al. Hippocampal volume in primary unipolar major depression: a magnetic resonance imaging study. *Biol Psychiatry* 2000;47:1087-90.
47. Bracht T, Linden D, Keedwell P. A review of white matter microstructure alterations of pathways of the reward circuit in depression. *J Affect Disord* 2015;187:45-53.
48. Cullen KR, Klimes-Dougan B, Muetzel R, et al. Altered white matter microstructure in adolescents with major depression: a preliminary study. *J Am Acad Child Adolesc Psychiatry* 2010;49:173-83.e1.
49. Murphy ML, Frodl T. Meta-analysis of diffusion tensor imaging studies shows altered fractional anisotropy occurring in distinct brain areas in association with depression. *Biol Mood Anxiety Disord* 2011;1:3.
50. Dalby RB, Frandsen J, Chakravarty MM, et al. Depression severity is correlated to the integrity of white matter fiber tracts in late-onset major depression. *Psychiatry Res* 2010;184:38-48.
51. Delorenzo C, Delaparte L, Thapa-Chhetry B, et al. Prediction of selective serotonin reuptake inhibitor response using diffusion-weighted MRI. *Front Psychiatry* 2013;4:5.
52. Jones DK. The effect of gradient sampling schemes on measures derived from diffusion tensor MRI: a Monte Carlo study. *Magn Reson Med* 2004;51:807-15.
53. Chen Y, Tymofiyeva O, Hess CP, et al. Effects of rejecting diffusion directions on tensor-derived parameters. *Neuroimage* 2015;109:160-70.
54. Fox MD, Raichle ME. Spontaneous fluctuations in brain activity observed with functional magnetic resonance imaging. *Nat Rev Neurosci* 2007;8:700-11.
55. Greicius MD, Flores BH, Menon V, et al. Resting-state functional connectivity in major depression: abnormally increased contributions from subgenual cingulate cortex and thalamus. *Biol Psychiatry* 2007;62:429-37.
56. Menon V. Large-scale brain networks and psychopathology: a unifying triple network model. *Trends Cogn Sci* 2011;15:483-506.
57. Menon V, Uddin LQ. Saliency, switching, attention and control: a network model of insula function. *Brain Struct Funct* 2010;214:655-67.
58. Seeley WW, Menon V, Schatzberg AF, et al. Dissociable intrinsic connectivity networks for salience processing and executive control. *J Neurosci* 2007;27:2349-56.
59. Schilbach L, Bzdok D, Timmermans B, et al. Introspective minds: using ALE meta-analyses to study commonalities in the neural correlates of emotional processing, social and unconstrained cognition. *PLoS One* 2012;7:e30920.
60. Schilbach L, Müller VI, Hoffstaedter F, et al. Meta-analytically informed network analysis of resting state fMRI Reveals hyperconnectivity in an introspective socio-affective network in depression. *PLoS One* 2014;9:e94973.
61. Dichter GS, Gibbs D, Smoski MJ. A systematic review of relations between resting-state functional-MRI and treatment response in major depressive disorder. *J Affect Disord* 2015;172:8-17.
62. Dutta A, McKie S, Deakin JFW. Resting state networks in major depressive disorder. *Psychiatry Res* 2014;224:139-51.
63. Wang L, Hermens DF, Hickie IB, et al. A systematic review of resting-state functional-MRI studies in major depression. *J Affect Disord* 2012;142:6-12.
64. Sheline YI, Barch DM, Price JL, et al. The default mode network and self-referential processes in depression. *Proc Natl Acad Sci U S A* 2009;106:1942-47.
65. Sheline YI, Price JL, Yan Z, et al. Resting-state functional MRI in depression unmasks increased connectivity between networks via the dorsal nexus. *Proc Natl Acad Sci U S A* 2010;107:11020.
66. Anand A, Li Y, Wang Y, et al. Antidepressant effect on connectivity of the mood-regulating circuit: an fMRI study. *Neuropsychopharmacology* 2005;30:1334-44.
67. Li B, Liu L, Friston KJ, et al. A treatment-resistant default mode subnetwork in major depression. *Biol Psychiatry* 2013;74:48-54.

68. Cullen KR, Klimes-Dougan B, Vu DP, et al. Neural correlates of antidepressant treatment response in adolescents with major depressive disorder. *J Child Adolesc Psychopharmacol* 2016;26:705-12.
69. Andreescu C, Tudorascu DL, Butters MA, et al. Resting state functional connectivity and treatment response in late-life depression. *Psychiatry Res* 2013;214:313-21.
70. Raichle ME, Snyder AZ. A default mode of brain function: a brief history of an evolving idea. *NeuroImage* 2007;37:1083-90.
71. Frodl T, Scheuerecker J, Schoepf V, et al. Different effects of mirtazapine and venlafaxine on brain activation: an open randomized controlled fMRI study. *J Clin Psychiatry* 2011;72:448-57.
72. Gyurak A, Patenaude B, Korgaonkar MS, et al. Frontoparietal activation during response inhibition predicts remission to antidepressants in patients with major depression. *Biol Psychiatry* 2016;79:274-81.
73. Williams LM, Korgaonkar MS, Song YC, et al. Amygdala reactivity to emotional faces in the prediction of general and medication-specific responses to antidepressant treatment in the randomized iSPOT-D trial. *Neuropsychopharmacology* 2015;40:2398-408.
74. Keedwell PA, Drapier D, Surguladze S, et al. Subgenual cingulate and visual cortex responses to sad faces predict clinical outcome during antidepressant treatment for depression. *J Affect Disord* 2010;120:120-5.
75. Toki S, Okamoto Y, Onoda K, et al. Hippocampal activation during associative encoding of word pairs and its relation to symptomatic improvement in depression: a functional and volumetric MRI study. *J Affect Disord* 2014;152–154:462-7.
76. Rizvi SJ, Salomons TV, Konarski JZ, et al. Neural response to emotional stimuli associated with successful antidepressant treatment and behavioral activation. *J Affect Disord* 2013;151:573-81.
77. Théberge J. Perfusion magnetic resonance imaging in psychiatry. *Top Magn Reson Imaging* 2008;19:111-30.
78. Vaccarino AL, Dharsee M, Strother SC, et al. Brain-CODE: a secure neuroinformatics platform for management, federation, sharing and analysis of multi-dimensional neuroscience data. *Front Neuroinform* 2018;12:28.
79. Marcus DS, Olsen TR, Ramaratnam M, et al. The Extensible Neuroimaging Archive Toolkit: an informatics platform for managing, exploring, and sharing neuroimaging data. *Neuroinformatics* 2007;5:11-34.
80. Gee T, Kenny S, Price CJ, et al. Data warehousing methods and processing infrastructure for brain recovery research. *Arch Ital Biol* 2010;148:207-17.
81. Farzan F, Atluri S, Frehlich M, et al. Standardization of electroencephalography for multi-site, multi-platform and multi-investigator studies: insights from the canadian biomarker integration network in depression. *Sci Rep* 2017;7:7473.
82. Hansen N, Coombs G, Deckersbach T, et al. MRI qualitative quality control manual. Cambridge (MA): Center for Brain Science; 2013. Available: http://cbs.fas.harvard.edu/science/core-facilities/neuroimaging/information-investigators/qc#qc_manual (accessed 2019 Feb. 14).
83. Fonov VS, Janke A, Caramanos Z, et al. Improved precision in the measurement of longitudinal global and regional volumetric changes via a novel MRI gradient distortion characterization and correction technique. *Proceedings of the 5th International Conference on Medical Imaging and Augmented Reality;* 2010 Sept. 19–20; Beijing. Berlin: Springer-Verlag; 2010:324-33.
84. Baker M, Penny D. Is there a reproducibility crisis? *Nature* 2016; 533:452-4.
85. Munafò MR, Nosek BA, Bishop DVM, et al. A manifesto for reproducible science. *Nature Human Behaviour* 2017;1:21.
86. Poldrack RA, Baker CI, Durnez J, et al. Scanning the horizon: towards transparent and reproducible neuroimaging research. *Nat Rev Neurosci* 2017;18:115-26.
87. Huffman JC, Celano CM, Beach SR, et al. Depression and cardiac disease: epidemiology, mechanisms, and diagnosis. *Cardiovasc Psychiatry Neurol*. 2013:695925.
88. Goodwin GM. Depression and associated physical diseases and symptoms. *Dialogues Clin Neurosci.* 2006;8(2):259-65.
89. Santesteban-Echarri O, MacQueen G, Goldstein BI, et al. Family functioning in youth at-risk for serious mental illness. *Compr Psychiatry* 2018;87:17-24.
90. Kennedy SH, Lam RL, Rotzinger S, et al. Symptomatic and functional outcomes and early prediction of response to escitalopram monotherapy and sequential adjunctive aripiprazole therapy in patients with major depressive disorder: a CAN-BIND-1 report. *J Clin Psychiatry*. 2019;80:18m12202.
91. Stuss DT. From silos to systems: an integrated approach to neuroscience innovation. *Nat Rev Drug Discov* 2015;14:295-6.